Materials Research Proceedings 41 (2024) 1259-1267 https://doi.org/10.21741/9781644903131-140

Analysis of oxidized hot working tool steel tribological behavior in tube piercing

MURILLO-MARRODÁN Alberto[1,a *], MERESSE Damien[2,b], GARCÍA Eduardo[1,c], MOREAU Philippe[2,d], LA BARBERA-SOSA Jose Gregorio[2,e] and DUBAR Laurent[2,f]

[1]Department of Mechanics, Design and Industrial Management, University of Deusto, 48007 Bilbao, Spain

[2]LAMIH UMR CNRS 8201, Université Polytechnique Hauts-de-France, F-59313, Valenciennes Cedex 9, France

[a]alberto.murillo@deusto.es, [b]damien.meresse@uphf.fr, [c]e.garcia@deusto.es, [d]philippe.moreau@uphf.fr, [e]josegregorio.labarberasosa@uphf.fr, [f]laurent.dubar@uphf.fr

Keywords: Friction, Hot Working Steel, Oxide Scale, Severe Contact Conditions

Abstract. In this paper the tribological behavior of the oxide layer present on the mandrel used in rotary piercing tube manufacturing operations has been analyzed. A hot upsetting sliding test campaign has been carried out in order to analyze the hot working steel oxide layer under different contact conditions. Optical microscopy, profilometry and XRD have been used to establish the type of contact and oxides generated, respectively. Results show abrasive sliding contact between mandrel and tube materials. Oxide transfer from the tube material to the mandrel material occurs in all the tested conditions. Regarding friction, the coefficient of friction COF is reduced by the presence of the oxide layer, confirming its lubricity. It has been observed how COF decreases with the increase of contact pressure and relative velocity. The value of COF is reduced from 0.42 to 0.18 if the contact pressure is increased from 165 to 200 MPa and the relative velocity is increased from 200 to 450 mm/s.

Introduction

In the rotary seamless tube piercing process, the tools are subjected to very demanding working conditions during their lifespan. The process is carried out at high temperature (the billet is heated, depending on the alloy, to values above 1200°C), high contact pressure and fast relative sliding velocities at billet-tool interfaces [1]. Of all the elements that make up the rolling-piercing mill, the mandrel, also known as the plug, is responsible for the generation of the hollow cavity of the pierced tube, starting from a solid billet. This is a critical element for the efficiency of the process and the final quality of the tube and, in addition, it is subjected to the most severe contact conditions. Therefore, special attention must be paid to the choice of the type of material to be used to design this tooling. In general, hot work tool steel, which contains Nickel, Chromium and Molybdenum as main alloying elements to improve its resistance to high temperatures and wear [2], is used when the material to be pierced is low carbon steel.

In order to improve the efficiency of the process and reduce its carbon footprint, one approach is improving the resistance of the tooling at high temperatures, reducing wear and friction. In the bulk metal forming field, lubricants are well extended, however, they have clear disadvantages from an environmental perspective as after forming, parts need to be cleaned and dried before going to subsequent stages [3]. Another alternative is the use of texturing, which can influence the friction coefficient and modify the material flow stress during the forming operation [4], but it does not improve substantially the wear performance. Furthermore, the use of coatings has been actively promoted in reducing wear in tooling systems for sheet metal forming operations as it can

prevent adhesive-related problems such as galling [5]. In the case of hot working tool steels, in contact with oxygen, metal surfaces can form oxide layers. When working in air at temperatures higher than 400 °C, the wear of the steels is typical oxidation wear [6]. In certain cases, these oxides can also serve as a protective barrier, preventing the steels from undergoing further oxidation. In addition, oxide layers can reduce metal-to-metal contact during the sliding motion of metal components, thus protecting them from wear [7].

The tribological behavior of the oxide layer resulting from the oxidation of hot work steels depends on many variables. A fundamental aspect is the type of oxide that makes up the tribo-layer. In the case of low carbon steels treated in air at high temperature, Zambrano et. al. [8] distinguished up to three types of iron oxide, namely Hematite, Magnetite and Wüstite. At room temperature, Hematite exhibits a hardness of approximately 1000 HV, leading to abrasive wear, while Magnetite, with a hardness of 500 HV in similar conditions, demonstrates a comparatively lower resistance. In contrast, Wüstite is renowned for its diminished hardness of 300 HV and stands out for possessing the highest lubricity among these oxides. As the temperature is increased to 900°C, some authors have reported hardness values for FeO, Fe_3O_4, and Fe_2O_3 of 105, 366, and 516 Hv, respectively [9]. In the case of Magnetite and Wüsite, these are the iron oxides that exhibit the highest ductility and resistance to wear at high temperature [10]. Typical morphology ratio reported at temperatures up to 1200°C is 95:4:1 (FeO:Fe_3O_4:Fe_2O_3) [11]. In addition, the thickness of the layer has been identified as a factor that severely affects the coefficient of friction, along with the temperature of the sample. A thick oxide scale produces a lower coefficient of friction, providing a certain degree of lubricity [12].

The presence of alloying elements in the steel also affects the oxide formation. Elements such as chromium, silicon or aluminum can enrich those oxide layers generated at the scale/substrate interface, leading to different mechanical properties and contact behavior. In addition, elements such as Ni or Cu, could increase the adherence of the oxides to the substrate, which increases the friction coefficient as oxides are not separating from the metallic interface, resulting in oxide-oxide contact [13].

In the case of hot rolling processes, several studies have focused on evaluating the effect of the oxide tribo-layer on the process. Pellizzari et al. [14] analysed the behaviour of high-speed steels and high chromium iron with regard to friction and wear at high temperature during hot rolling. Abrasion was identified as being caused by the oxide scale that develops on the hot carbon steel counterpart. Tieu et al. [15] determined that the rolling force and friction of pre-oxidised rolls are superior to those of virgin surface rolls for all thickness reductions and temperatures considered in their study. Utsunomiya et al. [16] identified that the relative sliding of the scale is the mechanism responsible for its apparent lubricating effect, and that the amount of the relative sliding increased with an increase in scale thickness. Nevertheless, one of the main challenges in examining the tribological behavior of a specific process is the lack of experimental procedure that effectively reproduces the forming process.

In this study, the tribological behavior of the oxide layer present on the mandrel used in rotary piercing tube manufacturing operations has been analyzed. A hot upsetting sliding test campaign has been carried out, which is able to reproduce industrial process contact conditions, including deformation during sliding contact. The contact of hot working tool steel with and without oxidation treatment has been evaluated and the type of contact and friction between tool-material assessed.

Materials and methods

The materials considered in this study are a high-strength low-alloy (HSLA) steel grade for the tube and a hot working tool steel for the plug. Both the tube and tool materials were provided by an industrial partner, and its chemical composition was evaluated in the laboratory. The chemical composition is listed in Table 1.

Table 1. Chemical composition (wt%) of tube and plug materials.

	C	Si	Mn	Cr	Ni	Mo	Cu	Al	Sn	Ti	V	N	Fe
Tube	0.236	0.24	1.03	0.16	0.09	0.06	0.26	0.003	0.01	0.043	0.043	0.01	rest
Plug	0.27	0.35	0.32	0.83	2.31	0.56	0.1	0.014	0.006	0.001	0.25	-	rest

The contactor (plug) and the specimen (tube) samples were machined directly from the interior of a plug and an as-cast billet, respectively. In order to prepare the contactor material in a comparable method to that used at industrial level, a one-hour oxidation treatment was carried out in a furnace at 700ºC with ambient air, which contained 21% oxygen, 78% nitrogen, with small amounts of carbon dioxide and other gases. In addition, some contactors without oxidation treatment were preserved. Regarding the specimen, it had no oxidation treatment. The microstructure and oxide layer after the heat treatment were assessed using optical microscopy. In Fig. 1a, it can be observed how the average oxide layer thickness resulted in approximately 11 µm. In Fig. 1b, the detail of the microstructure is shown. Some presence of martensite and bainite was observed, being mainly composed of acicular ferrite, with a hardness of 25 HRC.

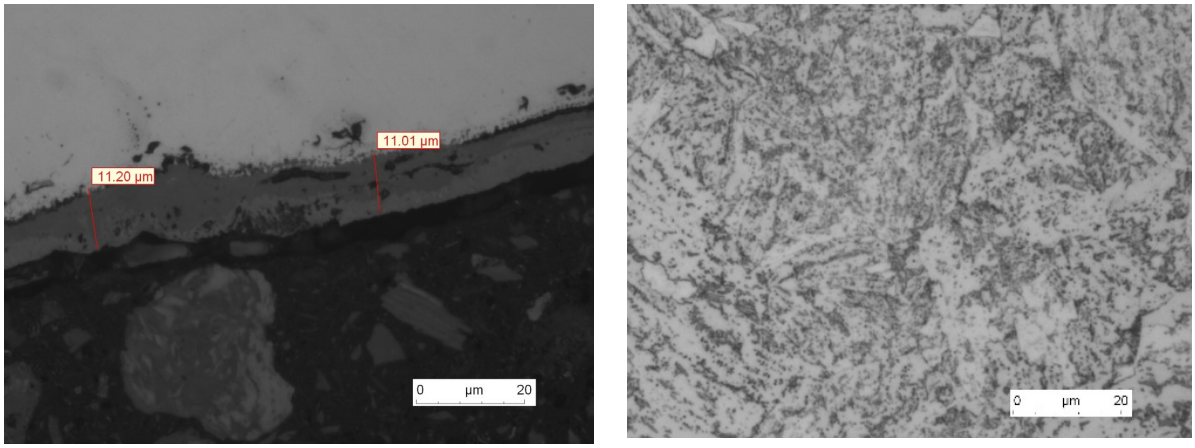

(**a**) (**b**)

Fig. 1. (a) Oxide layer in the contactor after the heat treatment and (b) material structure in the contactor.

The surface of the contactor was also assessed before performing the tribological tests. The roughness of the surface was Sa = 3.1 µm and, to characterize the composition of the tribo-layer, XRD tests were performed. Results revealed three different types of Iron-oxide, namely, Hematite, Magnetite and Wüstite. In addition, the presence of pure Iron and Chromium-Iron was identified. Regarding the specimen, heating tests were developed following the heating ramp used in the tests to assess the thickness of the oxide layer developed during the heating of this element into air. The mean thickness of the oxide layer was 500 µm.

The tribological testing campaign was carried out with the WHUST tribometer, by means of upsetting-sliding tests. During the test, the contactor (plug) penetrates the specimen (tube) and moves along the specimen surface while keeping the values of penetration and sliding velocity constant [17]. The geometries of the contact surfaces for the specimen and contactor were cylindrical with a radius of 15 mm and 10 mm, respectively. The physical tribometer and the schematic illustration of the test are shown in Fig. 2.

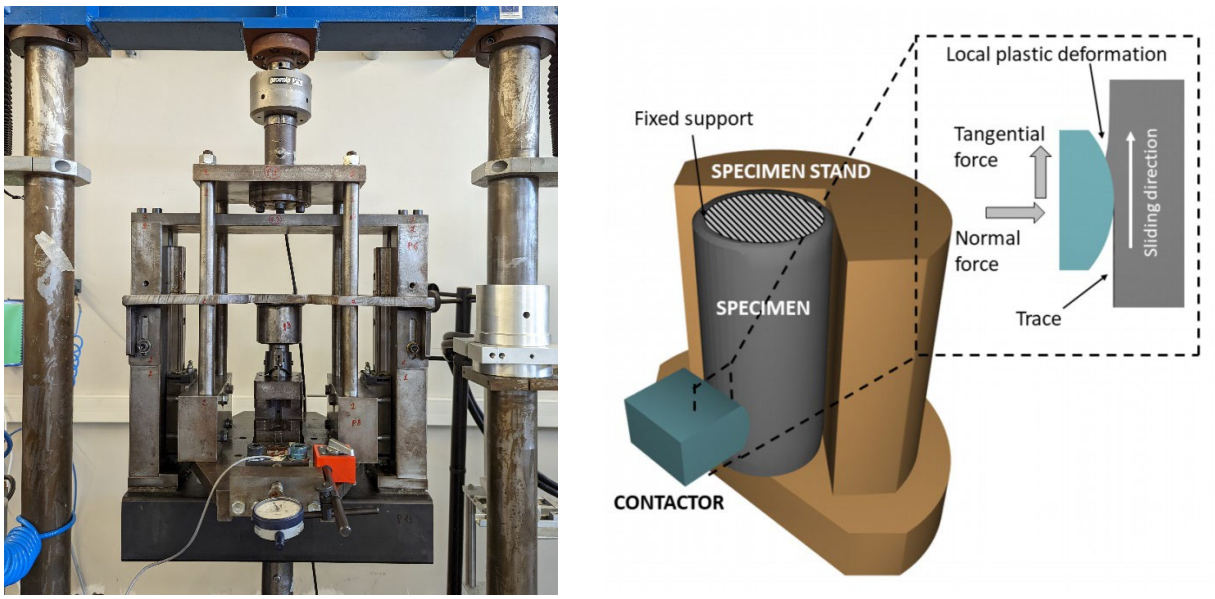

(a) **(b)**

Fig. 2 WHUST (a) tribometer set-up and (b) schematic illustration of the test.

In order to set the test conditions, temperature measures were carried out in an industrial piercing mill on the surface of the plug both, before and after piercing operation, yielding a maximum temperature of 450-500ºC. However, it is difficult to estimate this value experimentally since, depending on the size of the tube to be perforated, the heating can be higher or lower and, furthermore, when the plug is positioned between the rolls in the piercing mill is exposed to cooling fluid that reduces its initial temperature. Therefore, in order to estimate the surface heating of the mandrel during piercing, and to define the normal stress distribution at the contact, first, a FE simulation of the tube piercing process was carried out using Forge NxT software. From the results of the simulation, it was stated that in the contact temperature ranged from 275 to 475 ºC, the normal stress values were between 100 and 180 MPa. There was a high fluctuation in the sliding velocity, which showed minimum values of 150 mm/s at the tip of the plug and maximum values of 700 mm/s in the region with highest diameter (highest area reduction). In order to reproduce these conditions in the tribology tests, first the setup was simulated and different penetrations were tested. Finally, two penetrations (0.2 mm and 0.4mm) and two sliding velocities (200 mm/s and 450 mm/s) were defined, and three tests were performed for each condition.

The initial temperatures of the contactor and specimen were set to 250ºC and 1250ºC and, to reach them, a heating cartridge and an inductor system were used, respectively. The temperature in the surface contact is increased during the test reaching values up to 390ºC, depending on the configuration. In addition, three extra tests were performed at the maximum values of penetration and sliding velocity with the contactor what were not heat treated to generate the tribo-layer on their surface. The summary of all the tests performed is given in Table 2.

Table 2 Summary of the test conditions analysed in the WHUST tribometer.

Condition number	**Depth of penetration (mm)**	**Relative sliding velocity (mm/s)**	**Oxide layer in the contactor**
1	0.2	200	Yes
2	0.2	450	Yes
3	0.4	200	Yes
4	0.4	450	Yes
5	0.4	450	No

Results and discussion

Surface contact analysis. The contact analysis was performed by optical microscopy on the surface traces of the specimens and contactors after the test, as shown in Fig. 3. The specimen trace can be divided into three regions (see Fig. 3a), the third region has been excluded from the test since unwanted deformation of the specimen has occurred in this area due to the high contact pressure. This limits the usefulness of the tests after 30 mm displacement.

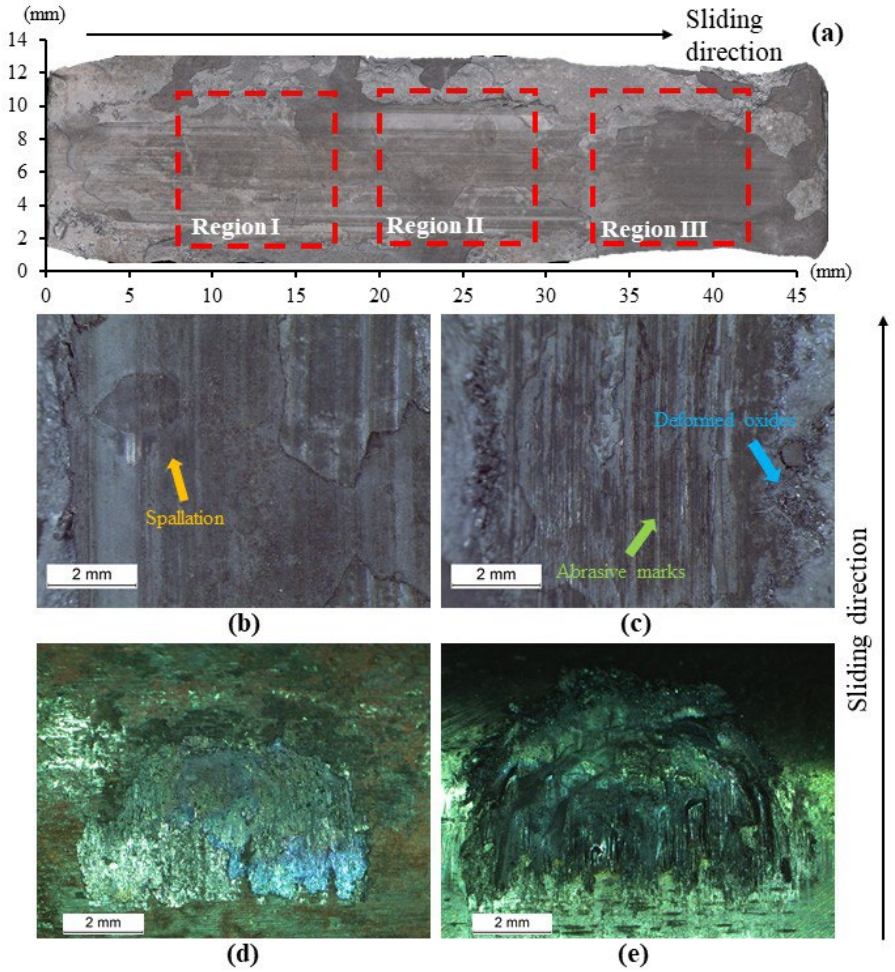

Fig. 3. (a) Trace of the specimen and optical microscopy of (b) specimen in test condition 4, (c) specimen in test condition 5, (d) contactor in test condition 4 and (e) contactor in test condition 5.

In Fig. 3b, no cracks are visible on the surface, although spallation of the oxides can be observed, the abrasion marks follow the sliding direction. Wear debris that have been welded to the surface of the trace are noted. In Fig. 3c, the abrasion marks are more pronounced. This condition corresponds to a metal/oxide contact. Furthermore, on the outer edges of the trace, scale debris that have been deformed and agglomerated on the surface of the specimen are noticed.

The result of the surface of the contactors after the test is shown in Figs. 3d and 3e. It can be noticed how there is transfer of oxides from the specimen to the surface of the contactors by means of adhesion mechanisms. The contactor in Fig. 3d was cross-sectioned, and no damage to the initial oxide layer was observed. A comparison of the two cases (contactor with and without oxide layer) reveals a higher amount of oxides transferred to the contactor without oxide layer. The reason behind the higher transfer may be caused by a higher degree of adhesion with the surface of the hot working steel, as well as the low adherence of the oxide layer generated on the specimen to

the substrate. No spallation of the oxide layer of the contactor, generated by the oxidation treatment, is visible. The presence of Nickel may explain the higher adhesion of the layer generated in the oxidizing treatment.

The wear tracks of the specimens shown in Fig. 3b and Fig. 3c (depth of penetration of 0.4mm and 450 mm/s of relative sliding velocity) were analyzed by means of focus variation techniques (Alicona). In Fig. 4, the profilometry of the trace of the aforementioned specimens, acquired across the sliding direction, is shown.

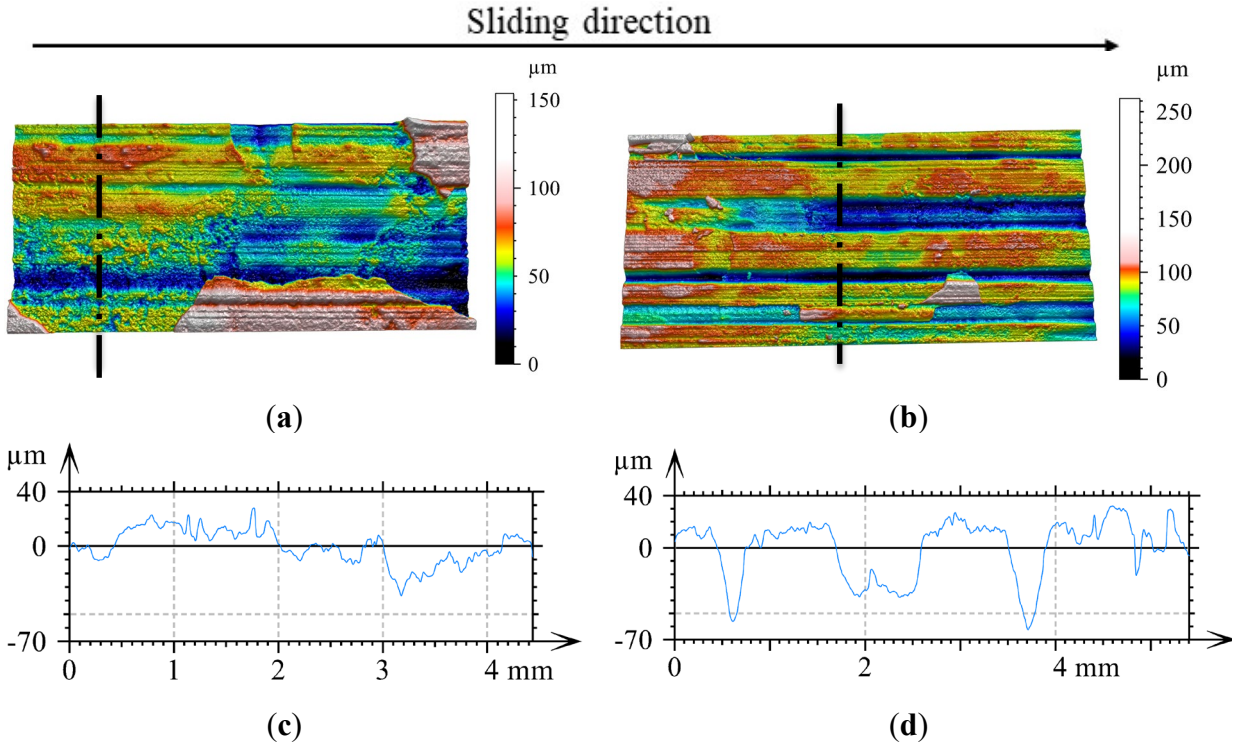

Fig. 4. Surface topography of (a) conditions 4 and (b) conditions 5, and transverse roughness profile of (c) conditions 4 and (d) conditions 5.

The surfaces were processed with Mountains®9 software, the areas of the trace corresponding to Region II have been extracted, and the level has been corrected by Least Square Plane Leveling (LSPL). In Fig. 4a, it can be seen how on the edges of the trace there are areas where the oxide has been spalled, while in the central zone some adhered wear debris alternate with marked valleys that indicate abrasion marks in the sliding direction of the sample. Regions where valleys show greater depth alternate with areas with less pronounced marks. In Fig. 5b, the abrasive wear marks are much more pronounced and remain throughout the entire area studied. In addition, some deformed and embedded oxides can be found on the surface. The surface roughness profiles of both conditions are shown in Figs. 5c and 5d. From their analysis, it can be stated that abrasive sliding wear is the dominating mechanism. During sliding, oxides tend to break and generate wear debris, and crushed oxides can be accumulated in the contactor yielding to oxide/oxide contact condition. From the analyzed profilometries and optical Fig.s, it's difficult to confirm if the test under condition 5 presents metal/oxide contact or oxide/oxide contact. In the case of condition 4, it can be identified as oxide/oxide.

Friction. Friction has been analyzed for all the conditions listed in Table 2. For each condition, three tests have been analyzed, obtaining a mean value for the friction factor *m* according to constant friction model, hereinafter referred as COF. The procedure to calculate COF depends on measured forces, contact penetration and length, not accounting for the material pile up [18]. In

addition, the evolution of COF throughout the displacement of the contactor along the specimen trace has been analyzed. Along the displacement, the first 5 mm of the trace are not useful since the specimen presents a chamfer, and after 30 mm, the results cannot be considered valid since some specimens showed unwanted deformation from that point onwards. Fig. 5 shows the evolution of COF with displacement for certain conditions, as well as the dependence of the COF with respect to relative velocity and contact pressure.

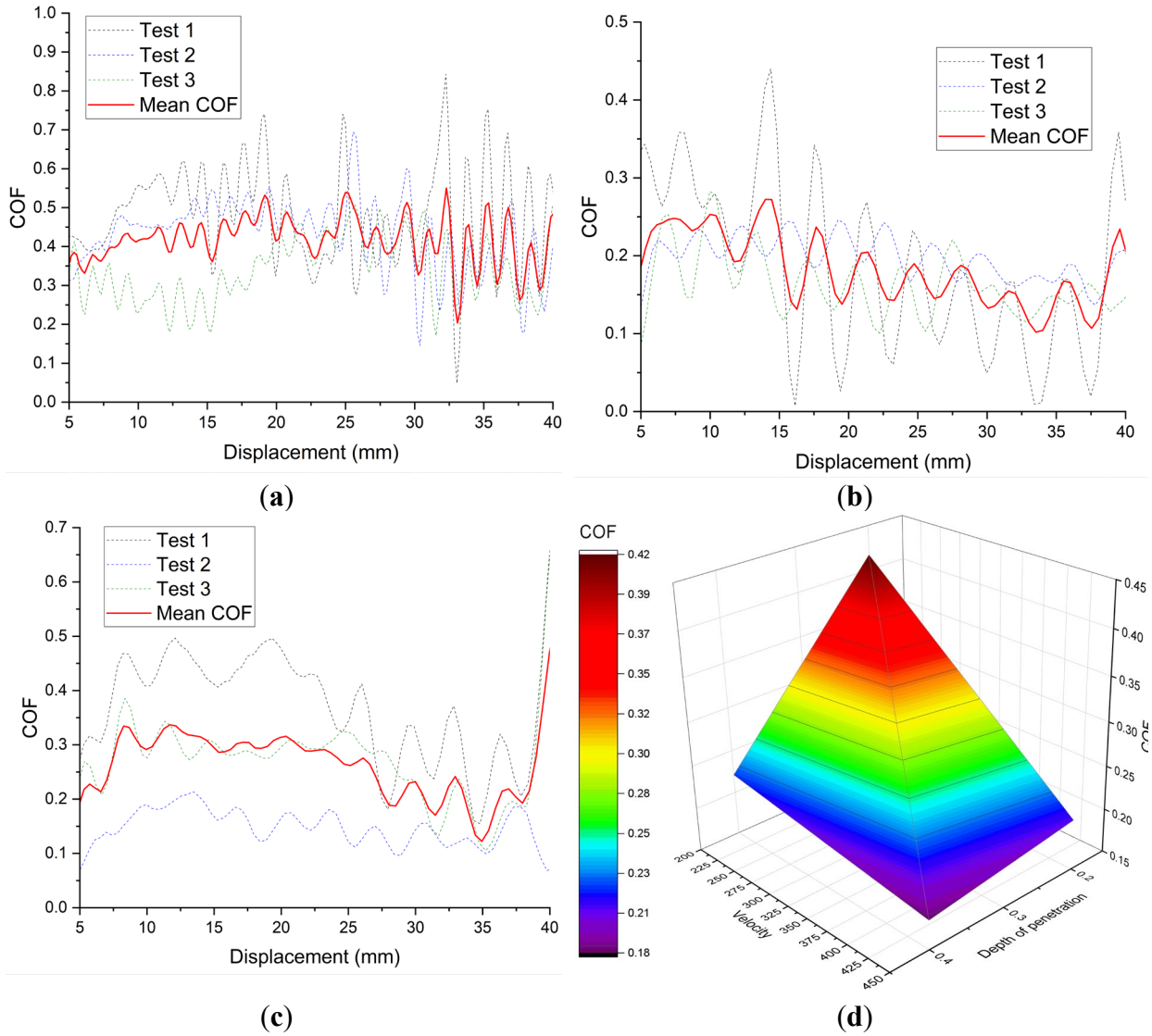

Fig. 5 COF evolution with displacement in (a) test conditions 1, (b) test conditions 4, (c) test conditions 5 and (d) COF evolution with sliding velocity and depth of penetration with the oxide layer in the contactor.

Fig.s 5a and 5b show the evolution of COF with displacement for condition 1 (low relative velocity and pressure) and condition 4 (high relative velocity and pressure), respectively. Both contactors have the oxidation treatment described in Sec. 2. The average COF at high contact pressure and relative speed is 0.18, while at conditions of low relative speed and contact pressure, it increases to a mean value of 0.42. Fig. 5c shows the evolution of the COF with displacement when the contactor does not have the oxidation treatment, under conditions of high relative velocity and pressure. The mean COF results in 0.28. If compared with its homologous case, it confirms that the presence of the oxide layer provides lubricity since COF has been increased from

0.18 to 0.28. Finally, in Fig. 5d, the mean COF results of cases 1 to 4 (all contactors are oxidation-treated) are represented in a surface, which makes COF dependent on the penetration depth (normal contact stress) and the relative sliding velocity. From the results, two clear trends can be observed. On the one hand, the increase in the relative sliding velocity yields a reduction in the COF. On the other hand, as higher contact pressures are applied, the COF is reduced. Among these two parameters, the COF shows greater sensitivity to changes in relative velocity at contact.

Conclusions

This study analyzes the tribological behavior of the oxide layer present on the mandrel used in rotary tube piercing operations. A hot upsetting sliding test campaign has been carried out. From the test results and their analysis, the following conclusions have been drawn:

- The oxide layer generated in the treatment is composed of Hematite, Magnetite and Wüstite. Its thickness is 11 microns and, in the tests, it has presented a good adhesion to the substrate without any apparent spalling.
- Adhesion of specimen oxides on the contactor surface occurred in all tested conditions. In the cases tested with oxidation treatment on the contactor this resulted in a type of oxide/oxide contact that was shown to be abrasive in nature.
- In the cases without oxidation treatment on the contactor, the sliding abrasion has been much more severe, showing grooves and abrasion marks of higher depth.
- Friction is lower when the contactor has the oxidation treatment, which confirms the lubricity of this layer.
- The COF value decreases with increasing relative velocity and contact pressure.

References

[1] Murillo-Marrodán A, García E, Barco J, Cortés F. Application of an Incremental Constitutive Model for the FE Analysis of Material Dynamic Restoration in the Rotary Tube Piercing Process. Materials 2020;13:4289. https://doi.org/10.3390/ma13194289.

[2] Zhang Y, Zhang C, Li F, Wang Z, Wang X, Wang C, et al. High-Temperature Oxidation Behavior of Cr-Ni-Mo Hot-Work Die Steels. Materials 2022;15:5145. https://doi.org/10.3390/ma15155145

[3] Cao J, Brinksmeier E, Fu M, Gao RX, Liang B, Merklein M, et al. Manufacturing of advanced smart tooling for metal forming. CIRP Annals 2019;68:605–28. https://doi.org/10.1016/j.cirp.2019.05.001

[4] Zhou R, Cao J, Wang QJ, Meng F, Zimowski K, Xia ZC. Effect of EDT surface texturing on tribological behavior of aluminum sheet. Journal of Materials Processing Technology 2011;211:1643–9. https://doi.org/10.1016/j.jmatprotec.2011.05.004

[5] Pelcastre L, Hardell J, Prakash B. Galling mechanisms during interaction of tool steel and Al–Si coated ultra-high strength steel at elevated temperature. Tribology International 2013;67:263–71. https://doi.org/10.1016/j.triboint.2013.08.007

[6] Wang SQ, Wei MX, Wang F, Cui XH, Chen KM. Effect of morphology of oxide scale on oxidation wear in hot working die steels. Materials Science and Engineering: A 2009;505:20–6. https://doi.org/10.1016/j.msea.2008.10.032

[7] Fontalvo GA, Mitterer C. The effect of oxide-forming alloying elements on the high temperature wear of a hot work steel. Wear 2005;258:1491–9. https://doi.org/10.1016/j.wear.2004.04.014

[8] Zambrano OA, Coronado JJ, Rodríguez SA. Mechanical properties and phases determination of low carbon steel oxide scales formed at 1200°C in air. Surface and Coatings Technology 2015;282:155–62. https://doi.org/10.1016/j.surfcoat.2015.10.028

[9] Lundberg S-E, Gustafsson T. The influence of rolling temperature on roll wear, investigated in a new high temperature test rig. Journal of Materials Processing Technology 1994;42:239–91. https://doi.org/10.1016/0924-0136(94)90181-3

[10] Dohda K, Boher C, Rezai-Aria F, Mahayotsanun N. Tribology in metal forming at elevated temperatures. Friction 2015;3:1–27. https://doi.org/10.1007/s40544-015-0077-3

[11] Sheasby JS, Boggs WE, Turkdogan ET. Scale growth on steels at 1200°C: rationale of rate and morphology. Metal Science 1984;18:127–36. https://doi.org/10.1179/msc.1984.18.3.127

[12] Munther PA, Lenard JG. The effect of scaling on interfacial friction in hot rolling of steels. Journal of Materials Processing Technology 1999;88:105–13. https://doi.org/10.1016/S0924-0136(98)00392-6

[13] Beynon JH. Tribology of hot metal forming. Tribology International 1998;31:73–7. https://doi.org/10.1016/S0301-679X(98)00009-7

[14] Pellizzari M, Cescato D, De Flora MG. Hot friction and wear behaviour of high speed steel and high chromium iron for rolls. Wear 2009;267:467–75. https://doi.org/10.1016/j.wear.2009.01.049

[15] Tieu AK, Zhu Q, Zhu H, Lu C. An investigation into the tribological behaviour of a work roll material at high temperature. Wear 2011;273:43–8. https://doi.org/10.1016/j.wear.2011.06.003

[16] Utsunomiya H, Nakagawa T, Matsumoto R. Mechanism of oxide scale to decrease friction in hot steel rolling. Procedia Manufacturing 2018;15:46–51. https://doi.org/10.1016/j.promfg.2018.07.168

[17] Dubois A, Dubar M, Dubar L. Warm and Hot Upsetting Sliding Test: Tribology of Metal Processes at High Temperature. Procedia Engineering, vol. 81, 2014, p. 1964–9. https://doi.org/10.1016/j.proeng.2014.10.265

[18] Dubois A, Dubar M, Debras C, Hermange K, Nivot C, Courtois C. New environmentally friendly coatings for hot forging tools. Surface and Coatings Technology 2018;344:342–52. https://doi.org/10.1016/j.surfcoat.2018.03.055